JOURNAL OF CATALYSIS 128, 126–136 (1991)

Preparation and Benzene Hydrogenation Activity of Supported Molybdenum Carbide Catalysts

JAE S. LEE,[1] MI H. YEOM, KI. Y. PARK, IN-SIK NAM, JONG S. CHUNG, YOUNG G. KIM, AND SANG H. MOON*

*Department of Chemical Engineering, Pohang Institute of Science and Technology, and Research Institute of Industrial Science and Technology, P.O. Box 125, Pohang, Korea; and *Department of Chemical Engineering, Seoul National University, Seoul, Korea*

Received April 17, 1990; revised September 10, 1990

Alumina-supported molybdenum carbide catalysts have been prepared from MoO_3/Al_2O_3 by (i) reduction with H_2 followed by carburization, (ii) direct carburization with CH_4/H_2, and (iii) nitriding with NH_3 followed by carburization. The temperature required for the complete reduction of MoO_3/Al_2O_3 depended strongly on the reductant employed. Temperature-programmed reduction coupled with on-line mass spectrometry and X-ray diffraction revealed reactions involved in the reduction and carburization of MoO_3. The supported molybdenum carbide catalysts exhibited high catalytic activity in benzene hydrogenation comparable to those of Pt or Ru. Complete reduction of molybdenum was essential for the high activity. Metallic molybdenum was much less active and less stable than its carbides, probably due to too strong adsorption of benzene. © 1991 Academic Press, Inc.

INTRODUCTION

Molybdenum carbide has received attention as a potential substitute for noble metals, especially Ru, as a catalytic material (*1–4*). Because of high temperatures involved in preparation, it is difficult to prepare molybdenum carbide with high specific surface areas S_g. Recently, unsupported molybdenum carbide powders with S_g of 60–200 m^2g^{-1} have been prepared by a novel temperature-programmed method (*2*) and a topotactic solid transformation method (*3, 5*). These carbides could also be made without free carbon or oxygen contaminating surface, an attribute required for efficient catalysts. These novel materials indeed showed excellent catalytic activity comparable to Ru in *n*-butane hydrogenolysis and CO hydrogenation (*4, 6, 7*).

Preparation of supported molybdenum carbide is more difficult because a strong interaction between molybdenum oxide and usual support materials such as silica or alumina dictates extremely high reduction temperatures. To avoid this problem, Nakamura *et al.* (*8, 9*) employed $Mo(CO)_6$ as a catalyst precursor which was deposited onto a dehydroxylated alumina and then decomposed in H_2 at 1220 K to yield metallic molybdenum clusters. Although $Mo(CO)_6$ is initially zerovalent and hence does not need reduction, the authors employed the high decomposition temperature to remove essentially all the carbon from the system. Lee *et al.* (*4*) carburized this Mo/Al_2O_3 with CH_4/H_2 to obtain Mo_2C/Al_2O_3. They also found that Mo/Al_2O_3 and Mo_2C/Al_2O_3 showed similar values of turnover rates (based on sites titrated by CO chemisorption) in *n*-butane hydrogenolysis (*4*) and CO hydrogenation (*6*) that were comparable to those on Ru. More recently, Chung *et al.* (*10, 11*) reported a simpler method of preparing a metallic Mo supported on Al_2O_3 by reduction of MoO_3/Al_2O_3 with H_2 at 1220 K. A striking feature of this preparation is that even under such a high reduction tempera-

[1] To whom correspondence should be addressed.

0021-9517/91 $3.00

ture, Mo did not sinter badly and small Mo particles with an average diameter of 4 nm were obtained.

In the present study, we report simple methods of preparing supported molybdenum carbide using MoO_3/Al_2O_3 as a precursor. Three methods of preparation were examined. The first method adopted the method of Chung *et al.* to prepare Mo/Al_2O_3 and then transformed it to carbide by a carburization at 950 K. The last two methods are based on the experience in preparing unsupported molybdenum carbide powders (*2, 3, 5*). Thus MoO_3/Al_2O_3 is either directly carburized in CH_4/H_2 or first nitrided in NH_3 to obtain Mo_2N, and then carburized. The characteristics of these supported molybdenum carbide were studied by X-ray diffraction (XRD) and CO chemisorption. The hydrogenation of benzene was studied over these catalysts and their activity compared with those of Pt and Ru.

EXPERIMENTAL

Catalyst Preparation

A γ-alumina (Alfa, 160 m^2g^{-1}) was impregnated with a solution of ammonium heptamolybdate (Alfa), dried at 270 K for at least 8 h, and calcined in air at 770 K for 5 h to obtain MoO_3/Al_2O_3. The MoO_3 loading was fixed at 5 wt% as Mo in all cases. This oxide was transformed to carbide by three methods: (i) reduction in H_2 at 1220 K for 2 h followed by carburization with a 20% CH_4/H_2 mixture at 950 K for 2 h, (ii) direct reduction/carburization in the 20% CH_4/H_2 mixture at 950 K for 2 h, (iii) nitriding in NH_3 at 970 K for 2 h followed by carburization in 20% CH_4/H_2 at 950 K for 2 h. These carbides are denoted as *M*–Mo_2C/Al_2O_3, D-Mo_2C/Al_2O_3, and N-Mo_2C/Al_2O_3, respectively. The temperature of carburization was chosen such that thermodynamics would not allow the deposition of graphitic carbon on the surface. The times required for the preparation were determined by monitoring with a quadruple mass spectrometer (MS, VG Micromass) the outlet of preparation cell and finding the times when the formation of water ceased. Preparation was performed in a typical atmospheric flow system made of Pyrex. Each preparation employed a quantity of 100 mg of MoO_3/Al_2O_3 loaded on a coarse quartz fritted disk in a cell which was designed to be used for preparation, adsorption, and catalytic reaction. A flow of reducing gases was maintained at 50 μmol s^{-1} by mass flow controllers. Methane (Matheson, 99.97%) and H_2 (Airco, 99.999%) were passed through a series of liquid nitrogen, 4A molecular sieve, and MnO/SiO_2 traps for purification before entering the cell. A furnace coupled to a controller maintained the temperature of the cell within ± 1 K, and a local thermocouple monitored the temperature of the sample. The 5% Ru/Al_2O_3 and 5% Pt/Al_2O_3 were prepared by an incipient wetness impregnation of the same alumina with solutions of hexaaminеruthenium(II) chloride and tetraamineplatinum(II) chloride hydrate respectively, and used as reference catalysts against which the performance of molybdenum carbide catalysts was compared.

Temperature-Programmed Reduction and X-Ray Diffraction

Although all the samples for adsorption and reaction study were prepared under isothermal conditions, temperature-programmed reduction (TPR) studies were performed to understand the characteristics of reduction processes. The MoO_3/Al_2O_3 was heated in He (Airco, 99.997%) at 870 K for 3 h in order to minimize the interference of water contained in alumina during the ensuing TPR. The temperature of the sample was raised at a linear rate of 0.33 K s^{-1} in a stream of reducing gas flowing at 50 μmol s^{-1}. Gaseous products were continuously monitored by MS. Powder XRD experiments were performed on a Rigaku Dmax-B diffractometer using Cu$K\alpha$ radiation to determine the bulk structure of the solid reactant, intermediates, and products. The intermediates were obtained by halting the TPR at intermediate temperatures. The samples were passivated before removing

from the preparation cell for the XRD measurement either by treating in flowing 1% O_2 in He for 5 h, or by opening a stopcock of the slightly pressurized cell and letting air to slowly diffuse in. Both procedures were found not to affect the bulk structure of molybdenum or molybdenum carbide samples seen by XRD. For comparison, the reduction behavior of unsupported MoO_3 (Alfa, 99.998%) was studied by the same TPR and XRD experiments. The amounts of MoO_3 in both supported and unsupported samples were kept equal.

CO Chemisorption and Benzene Hydrogenation

To measure CO chemisorption, the cell was isolated using stopcocks in the cell and transported to a volumetric adsorption system (Micromeritics Accusorb 2100E). The conventional adsorption and backadsorption method was employed at a desired adsorption temperature and the difference of the two isotherms extrapolated to zero pressure was taken as the amount of chemisorbed CO.

The hydrogenation of benzene was carried out at 323 K and atmospheric pressure. A flow (60 μmol s^{-1}) of H_2 was passed through two benzene saturators in series maintained at room temperature (RT) and 283 K, respectively, to obtain 6% benzene–H_2 mixture. The catalyst was never exposed to air before the reaction. The products were analyzed by an on-line gas chromatograph (HP 5890) equipped with a flame ionization detector and 2-m-long, 3.2-mm diameter Chromosorb W column.

RESULTS

Reduction of Unsupported and Supported Molybdenum Oxide

The gaseous products from temperature-programmed reduction of MoO_3/Al_2O_3 were analyzed by mass spectrometry (MS). Figure 1 shows the trend of water formation from reduction of MoO_3/Al_2O_3 by H_2, 20% CH_4/H_2, or ammonia. In order to minimize complications due to the water formed from dehydroxylation of alumina, all samples were heated in flowing He at 870 K for 3 h before TPR. This pretreatment, however, does not seem to remove the water from alumina completely as seen in Fig. 1a where TPR of pretreated alumina itself in H_2 shows a water peak near 1100 K. The TPR spectra in Fig. 1b–1d are not simple, but in general reduction appears to proceed in two stages. After the first peaks were observed, the TPR was halted at temperatures marked in Fig. 1, and the samples were examined by XRD. In all cases, the major intermediate phase was found to be MoO_2. At the end of the TPR, the product phases were, as expected, Mo, Mo_2C, and Mo_2N, respectively. TPR spectra were very similar except for the temperature required for complete reduction. The reduction by H_2 alone required the highest temperature followed by CH_4/H_2 and then by NH_3.

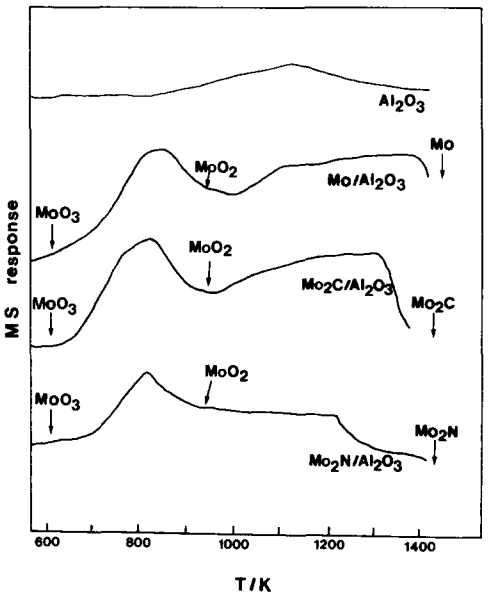

FIG. 1. The formation of water (m/e = 18) during temperature-programmed reduction of MoO_3/Al_2O_3; (a) alumina blank, (b) with H_2, (c) with 20% CH_4/H_2, and (d) with NH_3. Heating rate: 0.33 K s^{-1}. The solid phases determined by XRD are also indicated.

Figure 2 includes the TPR traces for the other gaseous products. For reduction with

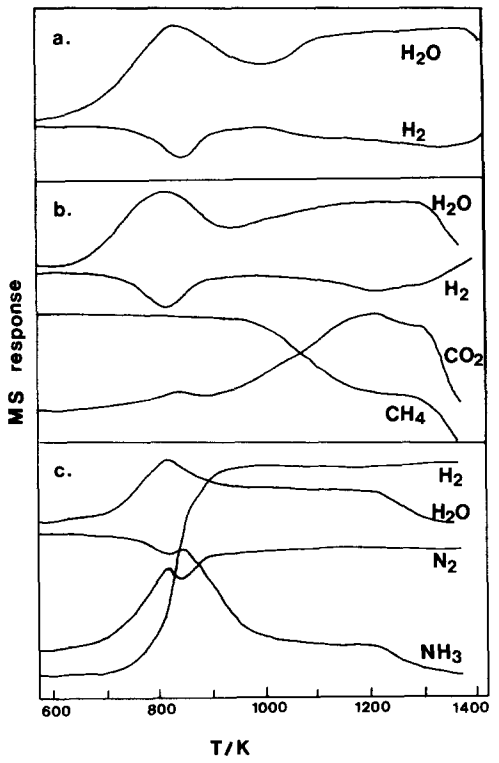

FIG. 2. Analysis by a mass sprectrometer of the gas phase during temperature-programmed reduction of MoO_3/Al_2O_3: (a) with H_2, (b) with 20% CH_4/H_2, and (c) with NH_3. Heating rate: 0.33 K s^{-1}. In all cases, the mass of molecular ions were followed.

H_2 (Fig. 2a), the trend of H_2 consumption agrees well with the trend of water formation throughout TPR. When a 20% CH_4/H_2 is used as reductant (Fig. 2b), methane remains unused in the first stage of reduction, but plays a major role in the second stage reduction to produce CO_2 and water. At higher temperatures, methane undergoes a reaction that produces H_2. With NH_3 (Fig. 2c), N_2 and H_2 were produced in addition to water.

The TPR spectra for unsupported MoO_3 are shown in Fig. 3 for comparison. These spectra for unsupported samples showed some features different from those for supported counterparts. Reduction of MoO_3 with H_2 and CH_4/H_2 required higher temperatures for the first stage but lower temperatures for complete reduction than MoO_3/Al_2O_3. Ammonia reduction occurred at greatly reduced temperatures. Like supported samples, all the intermediates were found by XRD to possess MoO_2 phase. The TPR spectra for other product gases from the reduction of MoO_3 were similar to those obtained for MoO_3/Al_2O_3 and, thus, are not shown.

Carburization of Molybdenum and Molybdenum Nitride

In order to prepare supported molybdenum carbide, the metallic molybdenum and molybdenum nitride intermediates must be carburized. Carburization of metallic molybdenum is known to be facile. Overbury (*12*) reported that noncarbidic surface carbon from the dissociative adsorption of ethylene on clean Mo(111) at RT transferred to a subsurface position by heating up to 600 K. Hence, our carburization temperature of 950 K is believed to be high enough to convert Mo/Al_2O_3 into Mo_2C/Al_2O_3 in 20% CH_4/H_2.

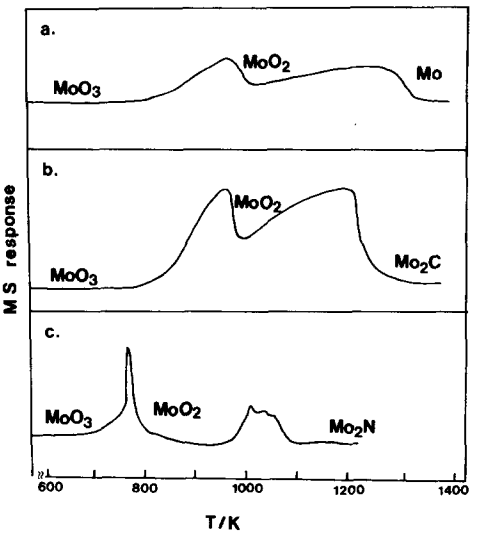

FIG. 3. The formation of water (m/e = 18) during temperature-programmed reduction of unsupported MoO_3: (a) with H_2, (b) with 20% CH_4/H_2, and (c) with NH_3. Heating rate: 0.33 K s^{-1}. The solid phases determined by XRD are also indicated.

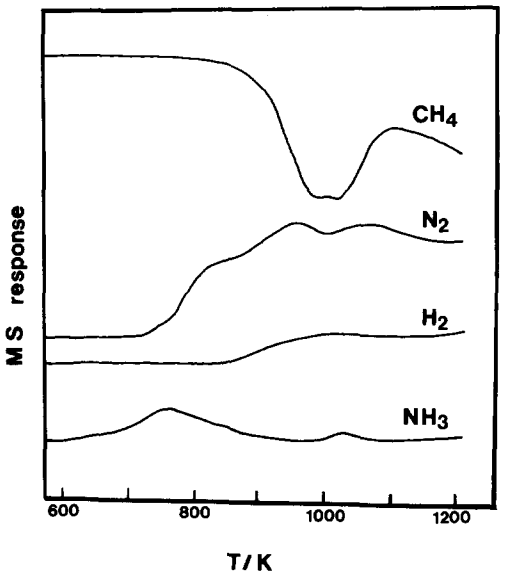

FIG. 4. Temperature-programmed reaction of Mo_2N/Al_2O_3 and 20% CH_4/H_2. Heating rate: 0.33 K s^{-1}.

The carburization process of molybdenum nitride was followed by TPR and the results are shown in Fig. 4. As expected, the main event of the process appears to be the exchange between N and C atoms. The presence of two ammonia peaks are probably due to a reaction between H_2 and surface nitrogen atom. Since N_2 and H_2 are present in the gas phase, the ammonia synthesis reaction between them is also possible. However, its contribution should be small due to unfavorable equilibrium at high temperatures. Increase in H_2 concentration above 850 K is due to decomposition of methane.

Characterization of Supported Molybdenum Carbides

Pretreated MoO_3/Al_2O_3 indicated the MoO_3 particles with the size of ca. 15 nm in XRD and its line broadening analysis (vide infra). As mentioned in the experimental section, three kinds of molybdenum carbides were prepared from this MoO_3/Al_2O_3 under isothermal conditions for catalytic reaction study. The XRD patterns for prepared carbides are shown in Fig. 5. The carbides prepared directly with CH_4/H_2 (D–Mo_2C/Al_2O_3) and through the metallic intermediate (*M*–Mo_2C/Al_2O_3) showed the structure of the hexagonal close-packed βMo_2C (*13, 14*). Meanwhile, the carbide through the nitride intermediate showed the structure of a face-centered cubic phase, called in literature αMoC_{1-x}, with x usually being close to $\frac{1}{2}$ (*3, 13, 14*). The widths of XRD peaks at half-maximum β were used to estimate the crystallite size D_c by means of the Scherrer equation $D_c = \lambda/(\beta \cos\theta)$, where λ represents the wavelength of Cu$K\alpha$ radiation (0.15418 nm) and θ the Bragg angle.

The chemisorption of CO shown in Table

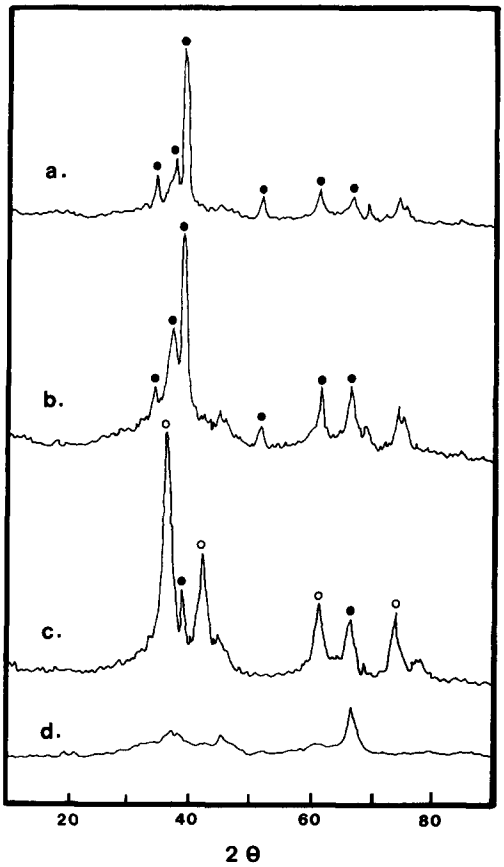

FIG. 5. The X-ray diffraction patterns of various molybdenum carbides: (a) *M*–Mo_2C/Al_2O_3, (b) *D*–Mo_2C/Al_2O_3, (c) *N*–Mo_2C/Al_2O_3, and (d) alumina. Major peaks were assigned for βMo_2C (●) and αMoC_{1-x} (○).

TABLE 1

Characteristics of Supported Molybdenum Carbides

Catalyst[a]	CO chemisorption/μmolg^{-1}		Particle Size/nm		% Metal exposed[d]
	At RT	At 196 K	D_c[b]	D_p[c]	
Mo/Al_2O_3	63	62	12.5	9.1	23.8
M–Mo_2C/Al_2O_3	94	144	9.0	7.8	27.6
N–Mo_2C/Al_2O_3	58	124	7.8	9.1	23.6
D–Mo_2C/Al_2O_3	80	122	11.0	9.0	23.5
Pt/Al_2O_3	52	57	—	—	22.3
Ru/Al_2O_3	67	74	—	—	15.0

[a] All catalysts contained 5 wt% metal.
[b] From X-ray diffraction.
[c] From CO chemisorption at 196 K and assuming spherical particles.
[d] From CO chemisorption at 196 K and assuming one-to-one chemisorption stoichiometry of CO and surface Mo atom except for Mo/Al_2O_3 where one CO molecule per two Mo atoms was assumed.

1 was measured at room temperature and 196 K, the latter maintained by a Dry ice–acetone bath. The alumina itself did not chemisorb significant amount of CO at RT, but chemisorbed 5–7 μmol g^{-1} at 196 K. The values in Table 1 were corrected for these blank runs. In general, approximately 60% more CO was chemisorbed on carbides at 196 K than at room temperature. The fraction of metal exposed to the surface was calculated from the data at 196 K assuming molecular adsorption of CO with one-to-one stoichiometry for carbides, and dissociative adsorption with a stoichiometry of one CO per two Mo atoms for Mo/Al_2O_3. Particle sizes were also calculated from the amounts of CO chemisorption at 196 K assuming spherical particles and a site density of 10^{15} cm^{-2}. Data for Pt and Ru used as reference catalysts are also shown.

Benzene Hydrogenation

The rate of benzene hydrogenation was expressed as site time yield (STY or average turnover rate), defined as the number of benzene molecules reacted per second per site titrated by CO chemisorption at 196 K. The change in STY at 323 K are shown in Fig. 6. The conversion of benzene was maintained below 10% for most cases. In all cases, cyclohexane was the only product. Initially, STY values over M–Mo_2C/Al_2O_3 and N–Mo_2C/Al_2O_3 were higher than those for Ru or Pt, but decreased rapidly with time on stream. This deactivation became more pronounced as the reaction temperature was increased. On the other hand, D–Mo_2C/

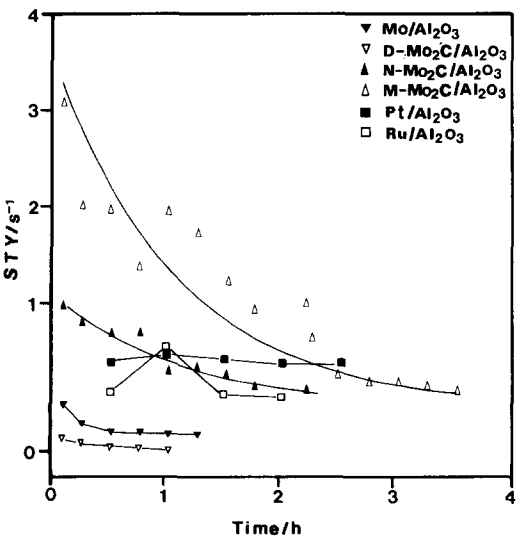

FIG. 6. Changes with time on stream in site time yield (STY) in the hydrogenation of benzene at 323 K and atmospheric pressure. The mole ratio of H_2/benzene of 15.7 was employed in all cases.

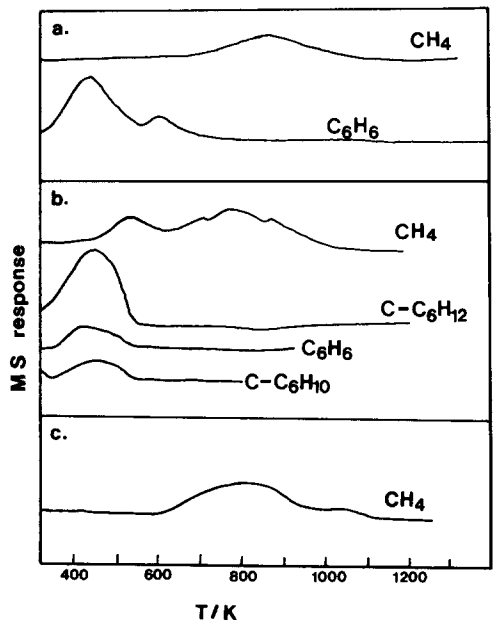

FIG. 7. Temperature-programmed reaction between H_2 (50 μmol s^{-1}) and Mo/Al_2O_3 (a) and M–Mo_2C/Al_2O_3 (b) used in benzene hydrogenation at 323 K for 3 h, and a fresh M–Mo_2C/Al_2O_3 (c). Heating rate: 0.33 K s^{-1}.

Al_2O_3 showed only a slight activity. The Mo/Al_2O_3 was much less active and less stable than active carbide catalysts.

After the benzene hydrogenation at 323 K for 3 h, some catalysts were treated in H_2 flow in a TPR mode and the resulting TPR spectra are shown in Fig. 7. On Mo/Al_2O_3, only benzene was desorbed until 700 K above which methane was detected (Fig. 7a). Comparing with TPR spectrum of clean M–Mo_2C/Al_2O_3 in Fig. 7c, the methane peak around 800 K could be assigned to the decomposition of bulk carbide. The TPR spectra for used M–Mo_2C/Al_2O_3 (Fig. 7b) are more complicated. In addition to a new methane peak near 550 K, cyclohexene and cyclohexane were also detected.

DISCUSSION

Reduction of Molybdenum Oxide on Alumina

The MoO_3/Al_2O_3 prepared in the present study was found by XRD to have MoO_3 crystallites with an average size of 15 nm. As brought to the attention of the authors by a referee, this is a rather large size for MoO_3 on alumina. It is well established that at Mo loadings corresponding to less than a monolayer, MoO_3 spreads over the alumina surface forming islands of less than two Mo atoms thick (*15*). Furthermore, it has been reported that heating a mechanical mixture of an active precursor (MoO_3 in the present case) and a carrier leads to the spontaneous dispersion of the precursor onto the support (*16*). Indeed, when our MoO_3/Al_2O_3 was calcined for 15 h instead of 5 h, the MoO_3 XRD patterns almost disappeared, indicating the spread of MoO_3 over the alumina surface. This particular sample appeared to undergo qualitatively the same solid transformations as for the sample containing 15 nm MoO_3 particles. The phases seen by XRD patterns and the gaseous products formed during the solid transformations were the same. The weak and broad XRD peaks for this new sample, however, indicated that generally much smaller particles of intermediates and products are formed from this well-dispersed MoO_3/Al_2O_3.

Reduction with H_2 of supported or unsupported MoO_3 has been the subject of many TPR studies (*2, 3, 17–21*). The reduction with other reductants has rarely been investigated. Furthermore, most of these previous studies tracked only the consumption of the reductant by a thermal conductivity detector and hence was difficult to reveal reactions involved in the reduction processes.

For MoO_3/Al_2O_3, Fig. 1 indicates that the first stage reduction is not affected by the reductant employed while the second stage reduction temperature was seriously affected. In case of reduction with CH_4/H_2, it was shown that the reductant responsible for the second stage reduction was CH_4 forming CO_2 and H_2O as the reduction product (Fig. 1b). This different reduction pathway may be responsible for facilitated reduction when CH_4/H_2 is used compared with the case of H_2 alone. Ammonia has

been found to be a more potent reductant than H_2 (*3, 5*), as reflected also in Fig. 1c. In all cases, the reduction proceeded through MoO_2 intermediate.

Unsupported MoO_3 also exhibits essentially the same reduction chemistry as the supported one. They show the same gaseous products and the same solid intermediate and products. The only difference is the temperature of reduction. The supported samples showed the first reduction peaks at lower temperatures. This could be attributed to the higher gas–solid interfacial areas for supported MoO_3. The size of supported MoO_3 was found to be 15 nm by XRD, while that of bulk MoO_3 was about 10 μm size as seen by a scanning electron microscopy (*3*). The higher temperatures required for the complete reduction for supported MoO_3 are believed to be due to an interaction with the alumina support. The extremely low temperature of initial reduction of bulk MoO_3 with ammonia is noteworthy. This effect has also been realized previously by other methods (*3, 5*).

In our TPR of supported and unsupported MoO_3, MoO_2 was the intermediate seen by XRD after the first stage of reduction irrespective of the reductant employed. On the contrary, Volpe and Boudart (*5*) found that, in TPR between unsupported MoO_3 and ammonia, MoO_3 transforms to MoO_2 and a highly dispersed molybdenum oxynitride phase with the latter in a dominant proportion. They showed that this oxynitride phase was responsible for the formation of the high surface area Mo_2N upon complete nitriding. Lee *et al.* (*3*) also observed a highly dispersed oxycarbide intermediate in Pt-catalyzed reduction/carburization of MoO_3 with CH_4/H_2. The formation of MoO_2 as the major intermediate in the present work appears to have originated from the rapid heating in TPR. The previous works employed 33 times slower rate of heating than that we used and found that this slow TPR was essential for the formation of high surface area products. Hence, the slow TPR is believed to have been essential for the formation of oxynitride or oxycarbide intermediate as well.

From the results of TPR studies on MoO_3 reduction (Figs. 1–3) and subsequent carburization (Fig. 4), and from XRD of solid phases, the reactions involved in these processes could be proposed as in Table 2. The reactions involved are obvious and well known for H_2 reduction. However, they appear very complicated when CH_4 or ammonia is involved. It is almost impossible to determine the exact stoichiometry of these complicated reactions based only on the results reported here. Hence, for some complicated reactions, the products were listed in parenthesis in Table 2 without their stoichiometric coefficients. The most serious obstacle to the determination of the stoichiometry is that the phase determined by XRD does not represent the composition of the whole solids. In particular, there may exist poorly crystalline phases which have escaped detection by XRD.

Characteristics of Supported Molybdenum Carbide Catalysts

As mentioned earlier, the molybdenum carbide samples used for the benzene hydrogenation were prepared under isothermal conditions. Before reaction, these samples were characterized by CO chemisorption and XRD. The XRD patterns of M–Mo_2C/Al_2O_3 and D–Mo_2C/Al_2O_3 show well-defined patterns of hexagonal βMo_2C phase. However, N–Mo_2C/Al_2O_3 exhibits mostly cubic αMoC_{1-x} phase contaminated by βMo_2C. Hence, the solid transformations involved in supported MoO_3 to carbide are essentially the same as those reported previously for bulk MoO_3 (*2, 3*). Thus the cubic phase which is metastable under the present preparation conditions has just been inherited from the cubic Mo_2N intermediate. This identification entitles the nitride-to-carbide transformation to be called "topotactic" (*3, 22*). The source of βMo_2C impurity may be the small amount of metallic intermediates which might have been formed during the nitride-to-carbide transformation. In Fig. 4,

TABLE 2

Reactions Involved in the Preparation of Mo_2C/Al_2O_3[a]

M-Mo_2C/Al_2O_3

(1) Mo/Al_2O_3 preparation

$MoO_3 + H_2 = MoO_2 + H_2O$ (The first stage reaction)

$MoO_2 + 2\ H_2 = Mo + 2\ H_2O$ (The second stage reduction)

(2) Carburization of Mo/Al_2O_3

$2\ Mo + CH_4 = Mo_2C + 2\ H_2$

D-Mo_2C/Al_2O_3

$MoO_3 + H_2 = MoO_2 + H_2O$ (The first stage reduction)

$MoO_2 + CH_4 = Mo_2C + (CO_2 + H_2O + H_2)$ (The second stage reduction and carburization)

$CH_4 = C + 2\ H_2$ (Carbon deposition)

N-Mo_2C/Al_2O_3

(1) Mo_2N/Al_2O_3 preparation

$MoO_3 + NH_3 = MoO_2 + (H_2O + N_2 + H_2)$ (The first stage reduction)

$MoO_2 + NH_3 = Mo_2N + (H_2O + N_2 + H_2)$ (The second stage reduction and nitration)

$NH_3 = 1/2\ N_2 + 3/2\ H_2$ (Ammonia decomposition)

(2) Carburization of Mo_2N/Al_2O_3

$Mo_2N + CH_4 = Mo_2C + 1/2\ N_2 + 2\ H_2$ (Carburization)

$N_2 + 3\ H_2 = 2\ NH_3$ (Ammonia synthesis)

$CH_4 = C + 2\ H_2$ (Carbon deposition)

[a] For reactions whose stoichiometry is not clear, only the identity of products is listed in parentheses.

it can be seen that nitrogen atoms leave the solid either as N_2 or NH_3 before the carbon atoms take their place. This will create metallic Mo intermediate which transforms to βMo_2C upon further carburization.

In a study of CO chemisorption of a Mo(100) single crystal, Ko and Madix (*23*) found that at 200 K, CO chemisorbed dissociatively on the clean surface and molecularly on the carburized surface. In a temperature-programmed desorption of CO from the carburized surface, it was also found that substantial amount of CO desorbed below room temperature. Results of CO chemisorption in Table 1 agree well with these previous results for the single crystal. Because of this weak binding of CO on molybdenum carbides, it is recommended to measure CO chemisorption at 196 K instead of RT in order to titrate the number of exposed sites. On this basis, all molybdenum samples showed that about 25% of total metal atoms were exposed to the surface.

The particle sizes D_p estimated from the amount of CO chemisorption and assuming spherical shape were between 7 and 9 nm. Differences are observed between these particle sizes and crystallite sizes estimated from X-ray diffraction (D_c). The presence of some relatively large particles together with many smaller particles may have contributed to the generally larger D_c values except for N-Mo_2C/Al_2O_3. A drawback in estimating D_p from CO chemisorption is that the surface composition of the carbide may not be equal to its ideal stoichiometry. Both excess and deficiency of carbon from ideal stoichiometry would decrease the amount of CO chemisorption. Hence D_p values in Table 1 should be considered as upper limits of average particle sizes.

Hydrogenation of Benzene

The activity for benzene hydrogenation of Mo_2C/Al_2O_3 is compared in Fig. 6 with Pt and Ru, which are among the most active known catalysts for the reaction. The initial STY values of M-Mo_2C/Al_2O_3 and N-Mo_2C/Al_2O_3 catalysts are higher than Pt or Ru, although Mo_2C/Al_2O_3 catalysts deac-

tivate more rapidly. This marked deactivation of molybdenum carbide catalysts is an obvious obstacle that should be overcome in order for these new catalysts to be practically applied. However, their remarkable initial activities warrant further research efforts. The poor performance of D–Mo_2C/Al_2O_3 is believed to be due to the incomplete reduction of the catalyst. Although XRD indicated the formation of the bulk carbide and the amount of CO chemisorption was similar to those for other active carbide catalysts, some oxygen may have remained, probably, on the surface and inhibited the reaction. The TPR spectra in Fig. 1b also suggests that the reduction/carburization temperature of 950 K for 2 h might not be sufficient. As mentioned earlier, this temperature was chosen to avoid the deposition of graphitic carbon on the surface at higher temperatures (*2*). The difficulty of removing the last small amount of oxygen form molybdenum has been emphasized by Burwell (*24*).

There are only a limited number of studies of benzene hydrogenation on molybdenum catalysts. It has been reported (*25, 26*) that Mo/Al_2O_3 prepared by reduction of MoO_3/Al_2O_3 at 773 K for 2 h contained mostly Mo(IV) and was inactive in this reaction below 410 K. On the other hand, metallic molybdenum catalysts prepared by reduction in H_2 above 1173 K, or by decomposition of $Mo(CO)_6/Al_2O_3$ hydrogenate benzene under similar conditions (*27, 28*). For MoO_3/Al_2O_3 reduced at high temperatures, turnover rates based on total Mo were reported to be $1.1–53 \times 10^{-3}$ s^{-1} at 373 K depending on reduction conditions (*28*). The higher side of these values are comparable to our initial STY values of Mo/Al_2O_3 in Fig. 6.

There have been discussions in the literature on the active phase of initially metallic molybdenum during catalytic reactions involving hydrocarbon reactants (*4, 6, 11*). Chung and Burwell (*11*) showed that much greater portion of alkane pulses fed over metallic Mo yielded hydrogenolysis products with high turnover rates, rather than being deposited on the surface to form a carbide. However, *in situ* X-ray absorption studies by Lee *et al.* (*4, 6*) demonstrated the formation of a surface carbide during steady-state reactions of *n*-butane hydrogenolysis at 510 K and CO hydrogenation at 570 K. Hence, Mo itself may have good activities. Yet it is unstable under those steady-state reaction conditions and transforms to a carbide. In both reactions, initially carburized molybdenum carbide catalysts showed 2–4 times higher reaction rates per site than those for initially metallic catalysts (*6*), and hence are better catalysts. In the present study, the reaction temperature of 323 K is much lower than 600 K, the temperature at which noncarbidic surface carbon deposited on Mo(111) single crystal surface was transferred to a subsurface position to form a carbide (*12*). This inability to form a carbide may be responsible for the much greater difference in the rates of benzene hydrogenation between metallic and its carbides catalysts than for the rates of *n*-butane hydrogenolysis and CO hydrogenation.

In order to understand the origin of the lower activity and the faster deactivation of Mo/Al_2O_3 than for carbides, used Mo/Al_2O_3 and M–Mo_2C/Al_2O_3 were subject to TPR in H_2. The TPR spectra for M–Mo_2C/Al_2O_3 showed the presence of all conceivable surface species, namely, reactant (benzene), product (cyclohexane), potential reaction intermediate (cyclohexene) and carbon deposits. Meanwhile, only benzene was detected from Mo/Al_2O_3. The CH_4 peak around 800 K is not believed to be due to the formation of carbide during the reaction since the reaction temperature was too low for the carbide to be formed. It is more likely that the carbide has been formed during heating up for TPR. It thus appears that most of the surface of Mo/Al_2O_3 has been covered by benzene during the reaction. This could be a good example which demonstrates the difference between molybdenum and its carbide in binding energies of molecules involved in a reaction. Apparently,

metallic molybdenum is not a good catalyst compared to the carbide because it binds benzene too strongly. This relationship between binding energies of group 6 metals and their carbide and their catalytic activities has been first suggested by Leclercq et al. (*1*) and presents an example of the Sabatier's principle.

ACKNOWLEDGMENTS

This work has been supported by Korean Science and Engineering Foundation through a contract 88-03-1302.

REFERENCES

1. Leclercq, L., Imura, K., Yoshida, S., Barbee, T., and Boudart, M., *in* "Preparation of Catalyst II" (B. Delmon, P. Grange, P. A. Jacobs, and G. Poncelet, Eds.), p. 627. Elsevier, Amsterdam, 1978.
2. Lee, J. S., Oyama, S. T., and Boudart, M., *J. Catal.* **106,** 125 (1987).
3. Lee, J. S., Volpe, L., Ribeiro, F. H., and Boudart, M., *J. Catal.* **112,** 44 (1988).
4. Lee, J. S., Locatelli, S., Oyama, S. T., and M. Boudart, *J. Catal.* **125,** 157 (1990).
5. Volpe, L., and Boudart, M., *J. Solid State Chem.* **59,** 348 (1985).
6. Lee, J. S., Yeom, M. H., and Lee, D.-S., *J. Mol. Catal.*, **62,** L45 (1990).
7. Ranhotra, G. S., Bell, A. T., and Reimer, J. A., *J. Catal.* 108, 40 (1987).
8. Nakamura, R., Bowman, R. G., and Burwell, Jr., R. L., *J. Amer. Chem. Soc.* **103,** 673 (1983).
9. Nakamura, R., Pioch, D., Bowman, R. G., and Burwell, Jr., R. L., *J. Catal.* **93,** 388 (1985).
10. Chung, J.-S., Zhang, J. P., and Burwell, Jr., R. L., *J. Catal.* **116,** 506 (1989).
11. Chung, J.-S., and Burwell, Jr., R. L., *J. Catal.* **116,** 519 (1989).
12. Overbury, S. H., *Surf. Sci.* **184,** 319 (1987).
13. Mclune, W. F., Ed., "Powder Diffraction File, Inorganic Compounds." JCPOS, Swarthmore, 1980.
14. Toth, L. E., "Transition Metal Carbides and Nitrides." Academic Press, New York, 1971.
15. Hall, W. K., *in* "Proceedings of the 4th International Conference on the Chemistry and Uses of Molybdenum" (H. F. Barry and P. C. H. Mitchel, Eds.), p. 224. Climax Molybdenum Co., Ann Arbor, 1982.
16. Xie, Y., Gui, L., Liu, Y., Zhang, Y., Zhao, B., Yang, N., Guo, Q., Duan, L., Huang, H., Cai, X., and Tang, Y., *in* "Adsorption and Catalysis on Oxide Surfaces" (M. Che and G. C. Bond, Eds.), p. 139. Elsevier, Amsterdam, 1985.
17. Massoth, F. E., *J. Catal.* **30,** 204 (1973).
18. Gajardo, P., Grange, P., and Delmon, B., *J. Chem. Soc., Faraday Trans. 1* **76,** 929 (1980).
19. Yao, H. C., *J. Catal.* **70,** 440 (1981).
20. Thomas, R., van Oers, E. M., de Beer, V. H. J., Medema, J., and Moulijn, J. A., *J. Catal.* **76,** 241 (1982).
21. Arnoldy, P., de Jonge, J. C. M., and Moulijn, J. A., *J. Phys. Chem.* **89,** 517 (1985).
22. Volpe, L., and Boudart, M., *Catal. Rev.-Sci. Eng.* **27,** 515 (1985).
23. Ko, E. I., and Madix, R. J., *Surf. Sci.* **109,** 221 (1981).
24. Burwell, Jr., R. L., *J. Catal.* **113,** 567 (1988).
25. Aboul-Gheit, A. K., and Cosyns, J., *J. Appl. Chem. Biotechnol.* **26,** 536 (1976).
26. Redey, A., and Hall, W. K., *J. Catal.* **108,** 185 (1987).
27. Chappen, J., and Brenner, A., *in* "9th North America Meeting of the Catalysis Society." Houston, TX, 1985.
28. Redey, A., Goldwasser, J., and Hall, W. K., *J. Catal.* **113,** 82 (1988).